

BLOCK POLYELECTROLYTE MICELLES/PROTEIN MIXED NANOSTRUCTURES IN AQUEOUS MEDIA

*Maria Karayianni and Stergios Pispas**

Theoretical and Physical Chemistry Institute, National Hellenic Research Foundation,
Athens, Greece

ABSTRACT

The interactions between a globular protein, hen egg white lysozyme (HEWL), and star-like block polyelectrolyte micelles formed by the self-assembly of a poly(tert-butylstyrene)-*b*-poly(sodium(sulfamate-carboxylate)isoprene) (PtBS-SCPI) amphiphilic diblock copolymer were studied in aqueous solutions. Due to the opposite charges present in HEWL (positive charges) and on the SCPI polyelectrolyte coronas of the block copolymer micelles (negative charges), nanostructured hierarchical complexes are formed at neutral pH and low ionic strength. Structure and properties of the complexes were investigated by means of dynamic, static and electrophoretic light scattering, as well as atomic force microscopy.

The solution behaviour, structure and effective charge of the formed nanoscale complexes proved to be dependent on the ratio of the two components. Presumably block polyelectrolyte micelles with a PtBS core and a SCPI corona decorated with HEWL molecules are initially formed. Moreover, the degree of charge neutralization caused by complexation determines the conformation and solubility of the complexes. Complexation of the macromolecular components at higher solution ionic strengths led to complexes of lower mass and nearly constant size. Such behavior may be correlated to the polyelectrolyte nature of the components. The structural investigation of the complexed protein by fluorescence and infrared spectroscopy revealed no signs of HEWL denaturation upon complexation.

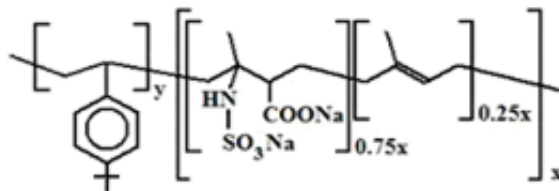
Keywords: Polyelectrolyte block copolymer micelles, protein-polyelectrolyte complexation, macromolecular self-assembled nanostructures, light scattering

* Correspondence/Reprint request: Dr. Stergios Pispas, Theoretical and Physical Chemistry Institute, National Hellenic Research Foundation, 48 Vassileos Constantinou Avenue, 11635 Athens, Greece. E-mail: pispas@eie.gr.

1. INTRODUCTION

Polyelectrolyte block copolymers have attracted considerable scientific interest owing to their unique properties. Their most important asset is that they combine the structural characteristics of amphiphilic block copolymers, polyelectrolytes and surfactants. Therefore, they constitute an intriguing class of macromolecules and furthermore provide various possibilities for custom design. Due to their amphiphilic character polyelectrolyte block copolymers in aqueous solutions usually self-assemble into core-shell micelles with a hydrophobic core and a polyelectrolyte corona. This self-assembly process is affected by numerous parameters that concern both the primary chemical structure of the macromolecules, such as the degree of polymerization of each block and the dissociation of the charged groups of the polyelectrolyte block, as well as the solution parameters, namely the concentration, pH, temperature and ionic strength. The resulting polyelectrolyte block copolymer micelles can be regarded as stimuli-responsive nanoparticles, with potential use in various technological and pharmaceutical applications, since the polyelectrolyte nature of their corona renders them susceptible to the changes of the solution physicochemical parameters. Consequently, over the past decades polyelectrolyte block copolymers micelles have been the subject of systematic experimental and theoretical studies and the results have been extensively reviewed [1–5].

Furthermore, the polyelectrolyte corona of these micelles enables them to bind oppositely charged entities, such as ions, organic molecules, metal nanoparticles, surfactants or synthetic and biological macromolecules, through electrostatic interactions. Among the possible applications of such systems is the formulation of flocculants and stabilizers of colloidal dispersions, surface modifiers and biocompatible coatings, matrices for metal ions and metal nanoparticles, carriers of biologically active compounds and drugs, *etc* [6]. In this field of study numerous experimental investigations involve the interpolyelectrolyte complexation between polyelectrolyte block copolymer micelles and linear polyelectrolytes of opposite charge, which leads to the formation of different types of macromolecular self-assembled nanostructures, including soluble or insoluble complexes, multilayer nanoparticles, networks or even gels [7–12]. Equivalently, the interaction of polyelectrolyte micelles with double hydrophilic polyelectrolyte block copolymers can be used as a means of preparing three-layered core-shell-corona micellar complexes [13–15]. Of similar interest is the case of electrostatic interaction between synthetic or natural polyelectrolytes and proteins. Proteins are another category of natural polyelectrolytes with intriguing conformational properties and biological functions. Electrostatic interaction is employed in a vast variety of technological applications concerning protein encapsulation, immobilization, purification and separation, in the development of functional nanobiomaterials and bio-organic hybrids with potential use in nanobiotechnology, while its study provides valuable insight into the interactions between charged biomacromolecules that take place in several biological systems [16, 17]. Such studies have been successfully extended to the case of double hydrophilic block copolymer/protein systems in an effort to create sophisticated functional nanostructures [18–22]. However, a rather limited number of experimental investigations have been focused so far on the complexation of amphiphilic block copolymer micelles with a polyelectrolyte corona and proteins [23–26], although such systems may provide several new opportunities for nanostructure formation and advantageous properties.



Scheme 1. Molecular structure of the PtBS-SCPI polyelectrolyte block copolymer. The degrees of polymerization are $x \approx 702$ and $y \approx 121$, while the degree of functionalization of the SCPI block is about 75%.

In a parallel manner, the interaction of proteins with spherical polyelectrolyte brushes is also interesting due to the structural analogies between the colloidal and micellar polymeric nanoparticles [27–29].

In this work we employ dynamic, static and electrophoretic light scattering (DLS, SLS and ELS), along with atomic force microscopy (AFM) in order to examine the complexation process, as well as the structure and solution behavior of the nanosized complexes formed between poly(tert-butylstyrene)-*b*-poly(sodium(sulfamate-carboxylate)isoprene) (PtBS-SCPI) (molecular structure shown in Scheme 1) polyelectrolyte block copolymer micelles and hen egg white lysozyme (HEWL) protein. Additional spectroscopic evaluation of the HEWL conformation after complexation was conducted, by means of fluorescence and infrared (IR) measurements. The central goal of this study is to create novel self-assembled and functional hybrid synthetic/biological macromolecular nanostructures and enrich basic understanding on behavioral motifs, as well as widen the application potential of nanostructured polymeric colloidal systems.

In aqueous solutions the PtBS-SCPI amphiphilic diblock copolymer self-assembles into micelles with a hydrophobic PtBS core and a polyelectrolyte SCPI corona. The SCPI block constitutes a novel strong polyelectrolyte, since each functionalized monomeric unit carries two negatively charged groups at neutral pH, while at the same time displays some intrinsic hydrophobic character due to the presence of unfunctionalized isoprene segments [30]. Moreover, HEWL is an extensively studied small globular protein with enzymatic activity and a pH-dependent net positive charge at pH values smaller than its isoelectric point $pI \approx 11$ [31, 32]. Therefore, the complexation process and the structure and solution behavior of the formed complexes between the PtBS-SCPI micelles and HEWL have been studied at pH 7 as a function of the ratio of the two components (*i.e.* the concentration of the protein keeping the copolymer concentration constant) and the solution conditions with respect to the ionic strength. The structure of the complexed protein, which determines whether enzymatic activity can be preserved upon complexation, has been also investigated by means of fluorescence and infrared spectroscopy.

2. EXPERIMENTAL PART

2.1. Materials

Protein: HEWL (dialyzed, lyophilized powder) with a molecular weight of $M_r = 14.7$ kg/mol was purchased from Fluka and used without any further purification.

Synthesis of the PtBS-SCPI polyelectrolyte block copolymer: The polyelectrolyte block copolymer sample was prepared by a post-polymerization functionalization reaction between chlorosulfonyl isocyanate (CSI, from Acros) and the isoprene segments of the polyisoprene (PI) block of the precursor PtBS-PI diblock copolymer prepared by anionic polymerization, as described in detail elsewhere [33]. The copolymer utilized in this study has a weight average molecular weight $M_w = 164.6$ kg/mol, and the weight fractions of PtBS and SCPI blocks are approximately 12% and 88%, which correspond to degrees of polymerization of about 121 and 702 monomeric units, respectively. Therefore, the particular PtBS-SCPI copolymer is considered an asymmetric amphiphilic diblock copolymer. The SCPI polyelectrolyte block is characterized by high charge density at neutral pH, since it combines strongly charged pH independent SO_3^- groups with weak acidic COO^- groups, neutralized at $\text{pH} < 4$. Moreover, the extent of functionalization was found to be about 75 mole %, by means of potentiometric titrations, elemental analysis and ^{13}C -NMR. Thus, the polyelectrolyte block retains some hydrophobic character due to the presence of unfunctionalized PI segments. Finally, its structural resemblance to the natural polysaccharide heparin (as far as the functional polar groups are concerned) enables possible use in biomedical applications [34, 35].

Sample preparation: A pH 7 buffer solution was prepared, from NaOH and 5 mM sodium phosphate, with ionic strength $I = 0.01$ N. Stock solutions of the polyelectrolyte block copolymer and the protein were prepared by dissolving a weighed amount of the dialyzed sample in the appropriate volume of the buffer. Consequently, the PtBS-SCPI solutions were heated at 60°C overnight in order to achieve solubilization, while the HEWL solutions were left to stand at room temperature for the same period of time for better equilibration. The final concentrations of the PtBS-SCPI and HEWL solutions were 0.25 mg/ml and 0.5 mg/ml, respectively. The complexes were prepared by adding different amounts of the HEWL solutions to PtBS-SCPI solutions of the same volume and concentration, under stirring. Finally, appropriate volumes of buffer solutions were added, so as to achieve a constant final volume and ionic strength (equal to that of the buffer solution) for all solutions prepared. Thus, the concentration of PtBS-SCPI was kept constant throughout the series of solutions, while that of HEWL varied in order to control the required ratio of the two components (or equivalently the $[-]/[+]$ charge ratio of the mixture). The solutions of the complexes developed bluish tint or turbidity upon mixing, indicating the formation of supramolecular complexes. Subsequently, the solutions of the complexes were left for equilibration overnight, which in some cases resulted in precipitation, depending on the HEWL concentration.

For the ionic strength dependent light scattering measurements, the ionic strength of the solution was increased by the addition of appropriate aliquots of a 1 N NaCl solution at pH 7, to 1 ml of the previously prepared solution of the complexes. After each addition the solution was rigorously stirred and left to equilibrate for 15 min before measurement. Changes in solutes concentrations due to NaCl solution addition were taken into consideration in the analysis of the light scattering data.

2.2. Techniques

Dynamic and Static Light Scattering (DLS and SLS): Light scattering measurements were performed on an ALV/CGS-3 compact goniometer system (ALV GmbH, Germany), equipped

with an ALV-5000/EPP multi tau digital correlator, a He-Ne laser operating at the wavelength of 632.8 nm, and an avalanche photodiode detector. Buffer and sample solutions were filtered through 0.45 μm hydrophilic PTFE Millex syringe filters (Millipore) in order to remove any dust particles or large aggregates. The samples were loaded into standard 1 cm width Helma quartz dust-free cells and measurements were performed at a series of angles in the range 20-150°.

Dynamic light scattering (DLS) measurements were evaluated by fitting of the measured normalized time autocorrelation function of the scattered light intensity $g_2(t)$, related to the electric field time autocorrelation function $g_1(t)$ by the Siegert equation, $g_2(t) = 1 + \beta|g_1(t)|^2$, where β is the coherence factor, depending on the experimental conditions [36, 37].

The data were fitted either with the aid of the CONTIN analysis or the use of the second order cumulant expansion and the distribution of relaxation times τ or the mean relaxation rate $\Gamma = 1/\tau$, were obtained respectively. Furthermore, the cumulant analysis yields the size polydispersity index of the system $PDI = \mu_2/\Gamma^2$, where μ_2 is the second order coefficient of the expansion. Assuming that the observed fluctuations of the scattered intensity are caused by diffusive motions, the apparent diffusion coefficient D_{app} is related to the relaxation time τ as, $D_{app} = 1/\tau q^2$, where q is the scattering vector defined as $4\pi n_0 \sin(\theta/2)/\lambda_0$ with n_0 , θ and λ_0 the solvent refractive index, the scattering angle and the wavelength of the laser in vacuum respectively.

From the apparent diffusion coefficient D_{app} , the hydrodynamic radius R_h can be obtained, using the Stokes-Einstein relationship

$$R_h = \frac{k_B T}{6\pi \eta_0 D_{app}} \quad (1)$$

where k_B is the Boltzmann constant, T is the temperature and η_0 is the viscosity of the solvent.

Static light scattering (SLS) measurements were treated by the Zimm method using the equation

$$\frac{Kc}{\Delta R_\theta} = \frac{1}{M_w} \left(1 + \frac{1}{3} R_g^2 q^2 \right) + 2A_2 c \quad (2)$$

where M_w is the weight averaged molecular weight, R_g is the average radius of gyration, A_2 is the second osmotic virial coefficient, c is the polymer concentration, ΔR_θ is the corrected Rayleigh ratio, which depends on the polymer concentration c and the magnitude of the scattering vector q , and the constant factor K is given by the relationship

$$K = \frac{4\pi^2 n_0^2}{\lambda_0^4 N_A} \left(\frac{\partial n}{\partial c} \right)^2 \quad (3)$$

where n_0 , λ_0 , N_A are the refractive index of the solvent, the laser wavelength in vacuum, the Avogadro's number respectively and $\partial n / \partial c$ is the refractive index increment of the sample solution with respect to the solvent.

Electrophoretic Light Scattering (ELS): ζ -potential measurements were performed with a ZetaPlus Analyzer (Brookhaven Instruments) equipped with a 35 mW solid state laser, operating at $\lambda = 660$ nm. ζ -potential values were determined using the Smolukowski equation relating the ionic mobilities with surface charge, and are reported as averages of ten repeated measurements.

Atomic Force Microscopy (AFM): AFM measurements were performed on a Quesant Q-Scope 250 atomic force microscope (Quesant Instrument Co., USA) in the tapping mode, under ambient conditions. The instrument was equipped with a NSC16 silicon (W_2C Si_3N_4) cantilever, available from Quesant instruments, USA, having a typical force constant of 40 N/m, a cone angle of less than 20° and radius curvature less than 10 nm. Imaging was carried out with a 40- μ m Dual PZT scanner on different scanning areas, at a scanning rate of 3 Hz and with image resolution of 600x600 pixels in intermittent contact (broadband mode). The z axis calibration was performed by imaging a TGZ01 silicon grating with silicon oxide steps having height of 18.3 nm (Mikromasch Inc.). Samples for imaging were prepared by placing a drop of the aqueous solutions of the complexes onto fresh, dried silicon wafers, pre-cleaned with isopropanol. After keeping in contact for typically 5 to 10 min, excess water was bolted carefully by filter paper and samples were left to dry in air. In this way supramolecular structures were absorbed on the wafer surface from the same solutions investigated by light scattering for direct comparison.

Fluorescence spectroscopy: Steady-state fluorescence spectra of the tryptophan residues of the neat and complexed HEWL were recorded with a double-grating excitation and a single-grating emission spectrofluorometer (Fluorolog-3, model FL3-21, Jobin Yvon-Spex) at room temperature.

Excitation wavelength used was $\lambda = 290$ nm and emission spectra were recorded in the region 350-500 nm, with an increment of 1 nm, using an integration time of 0.5 s. Slit openings of 5 nm were used for both the excitation and the emitted beam. Under the employed experimental conditions fluorescence from the tryptophan residues of HEWL is observed and utilized to extract information on changes of the protein conformation. The neat PtBS-SCPI solution does not show any significant fluorescence.

Infrared spectroscopy (IR): Infrared spectra of the protein, polyelectrolyte block copolymer and complexes in thin film form were acquired at room temperature in the range 5000-550 cm^{-1} , using a Fourier transform instrument (Bruker Equinox 55), equipped with a single bounce attenuated total reflectance (ATR) diamond accessory from SENS-IR. A small aliquot of each solution was placed on the ATR element and dried under N_2 flow before measurement. For each sample the final spectrum is the average of three 100-scan measurements at 2 cm^{-1} resolution. The measurement of each sample was bracketed by two background spectra in order to allow for the elimination of H_2O vapor bands by interpolation.

3. RESULTS AND DISCUSSION

3.1. Characterization of the PtBS-SCPI Micelles

Dynamic and static light scattering (DLS and SLS) measurements were performed in order to characterize the PtBS-SCPI micelles.

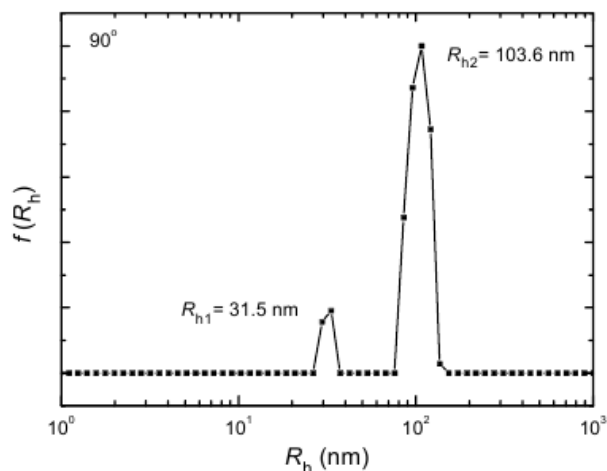


Figure 1. Hydrodynamic radius distributions from DLS measurements at 90° of a 0.083 mg/ml PtBS-SCPI solution at pH 7 and 0.01 N ionic strength.

Figure 1 shows the hydrodynamic radius (R_h) distributions obtained from the CONTIN analysis of DLS measurements at 90° , of a 0.083 mg/ml PtBS-SCPI solution at pH 7 and 0.01 N ionic strength. As it can be seen, the solution exhibits a main peak at high R_h values which apparently corresponds to the formed PtBS-SCPI micelles (R_{h2}) and a significantly smaller one at lower R_h values which most probably denotes the presence of a small number of free unimer diblock copolymer chains (R_{h1}) in the solution. The corresponding R_{h1} and R_{h2} values are 31.5 and 103.6 nm, respectively. Additionally, SLS measurements showed that the apparent weight average molecular weight of the micelles at pH 7 and 0.01 N ionic strength was $M_w \approx 1.6 \times 10^6$ g/mol, which denotes an aggregation number $N_{agg} \approx 10$, while the corresponding radius of gyration was $R_g \approx 107$ nm. It should be noted that the observed rather small N_{agg} of the micelles is a consequence of the highly asymmetric composition of the amphiphilic diblock copolymer chain, or in other words the high ratio of hydrophilic to hydrophobic monomeric units (~ 6) [38, 39].

3.2. Complexation of PtBS-SCPI Micelles and HEWL at pH 7 and 0.01 N Ionic Strength

Initially, the complexation process between the PtBS-SCPI polyelectrolyte micelles and HEWL at pH 7 and 0.01 N ionic strength was investigated by means of dynamic light scattering. At pH 7 the SCPI polyelectrolyte block carries two negatively charged groups per functionalized monomeric unit and HEWL has a net positive charge of +8, thus under these conditions electrostatically driven complexation is expected to readily occur. The obtained results from DLS measurements at 90° regarding the values of the light scattering intensity, I_{90} , the hydrodynamic radius, R_h , and the polydispersity index of the system, PDI , are shown in Figure 2, as a function of the protein concentration, C_{HEWL} , in the solutions of the complexes. The concentration of PtBS-SCPI copolymer is kept constant at 0.083 mg/ml throughout the series of solutions. In all cases, the point at zero protein concentration ($C_{HEWL} = 0$) denotes the corresponding value of the net PtBS-SCPI solution.

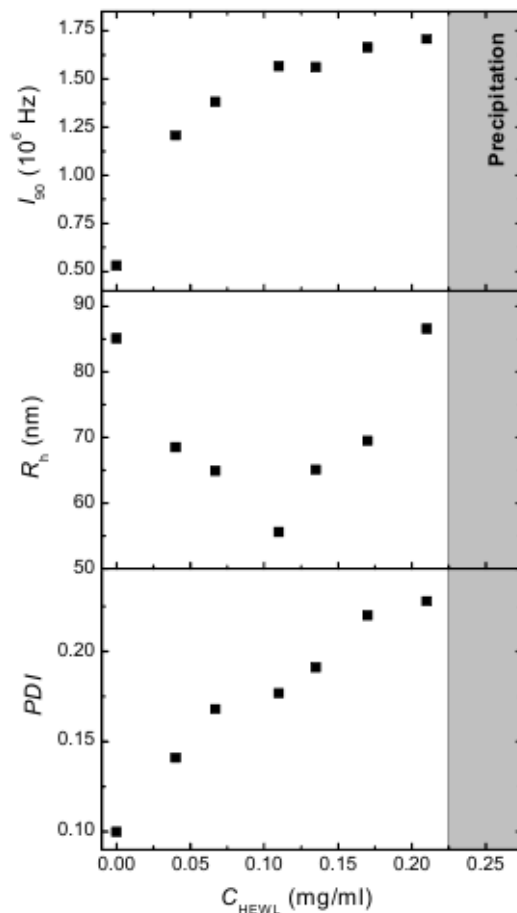


Figure 2. Light scattering intensity at 90° , I_{90} , hydrodynamic radius, R_h , and polydispersity index, PDI , as a function of C_{HEWL} , for the solutions of the PtBS-SCPI/HEWL system at pH 7 and 0.01 N ionic strength.

As observed, the value of the scattering intensity, I_{90} , which is proportional to the mass of the species in solution, increases abruptly upon the addition of the protein and continues to increase more gradually as a function of C_{HEWL} , providing proof of the occurring complexation. On the other hand, the hydrodynamic radius, R_h , of the complexes initially decreases up to $C_{\text{HEWL}} = 0.11$ mg/ml and subsequently increases. Moreover, the polydispersity index, PDI , shows increasing values as C_{HEWL} becomes higher. Finally, at high protein concentration precipitation of the solutions of the complexes takes place.

These changes suggest that upon the addition of HEWL to the PtBS-SCPI solution the protein molecules are complexed with the corona polyelectrolyte chains of the micelles. Complexation leads to neutralization of the charges on the SCPI polyelectrolyte block and thus to the weakening of the electrostatic repulsions. As a result the polyelectrolyte corona of the complexed micelles shrinks and their size decreases. As the protein concentration increases each polyelectrolyte chain interacts with an increasing number of protein molecules, which leads to a higher degree of charge neutralization and a further decrease of the size of the complexes. Nevertheless, the neutralization of the polyelectrolyte charges that takes place reduces the solubility of the formed complexes and causes their aggregation.

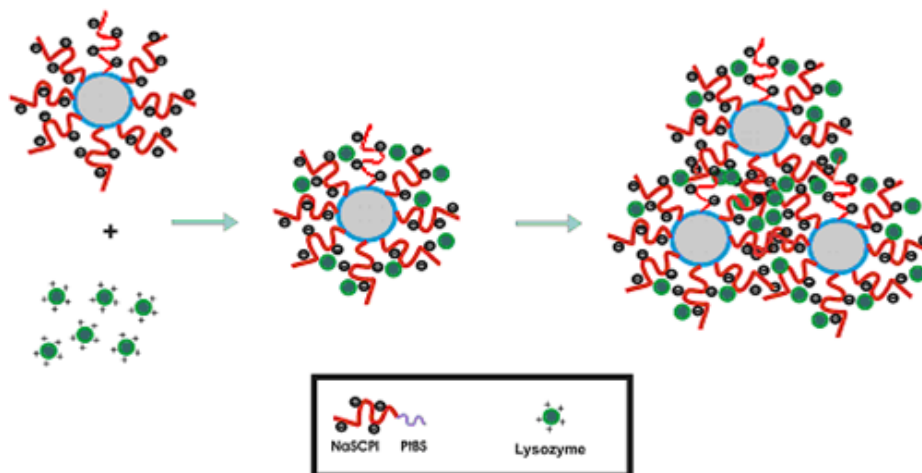


Figure 3. Schematic representation of the structure of the formed complexes as a function of C_{HEWL} , for the solutions of the PtBS-SCPI/HEWL at pH 7 and 0.01 N ionic strength.

The onset of the aggregation is marked by the transition to increasing R_h values. Actually, as the number of complexed protein molecules per polyelectrolyte chain becomes higher the aggregation is even more pronounced, *i.e.* each aggregate is comprised by a larger number of complexes. Eventually, the increase of the mass and size of the aggregates is so pronounced that they are no longer soluble and precipitation occurs. A schematic representation of the structure of the complexes is given in Figure 3.

As mentioned before in the PtBS-SCPI solution polyelectrolyte micelles and free unimer diblock copolymer chains were found to coexist. The effect of the protein addition on each population can be established from the hydrodynamic radius distributions of the complexes that are shown in Figure 4 for representative C_{HEWL} values. Obviously, in all cases two scattering populations are distinguished and the comparison with the distribution of the neat PtBS-SCPI solution, leads to the conclusion that these populations most probably correspond to the complexes formed by the protein molecules and the free unimer diblock copolymer chains or by protein and the polyelectrolyte micelles. Of course the latter species is the main population in all the solutions of the complexes. However, the size of both types of complexes changes in a similar manner and in accordance to the R_h values transition of Figure 1. An initial decrease is observed as a consequence of the shrinking of the polyelectrolyte chains caused by their complexation with the protein molecules, while further increase of the protein concentration provokes the aggregation of both types of complexes, which is expressed as an increase of their size. It should be noted that the R_h values in Figure 1 have been estimated using cumulants analysis, which yields a weighted average of all scattering species in solution and as a result are somewhat smaller than the corresponding values derived from the hydrodynamic radius distributions.

Multangle light scattering measurements allowed for the determination of the ratio R_g/R_h for the complexes in all cases, where R_g is the radius of gyration of the nanostructures in solution. The ratio provides information on the shape of the particles formed by block polyelectrolyte micelles/protein complexation. Values of R_g/R_h were in the range 0.77 – 0.93 indicating a spherical shape for the PtBS-SCPI/HEWL complexes at all compositions investigated.

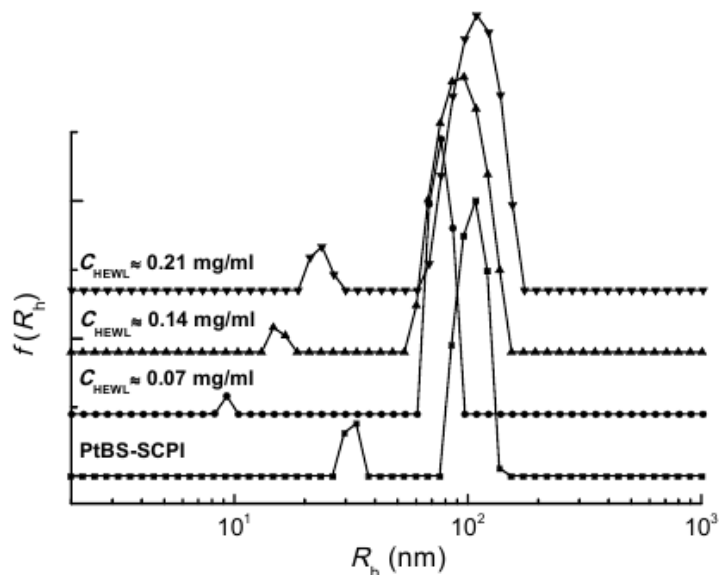


Figure 4. Hydrodynamic radius distributions at 90° for representative C_{HEWL} values, for the solutions of the PtBS-SCPI/HEWL system at pH 7 and 0.01 N ionic strength. The corresponding PtBS-SCPI distribution is included for comparison.

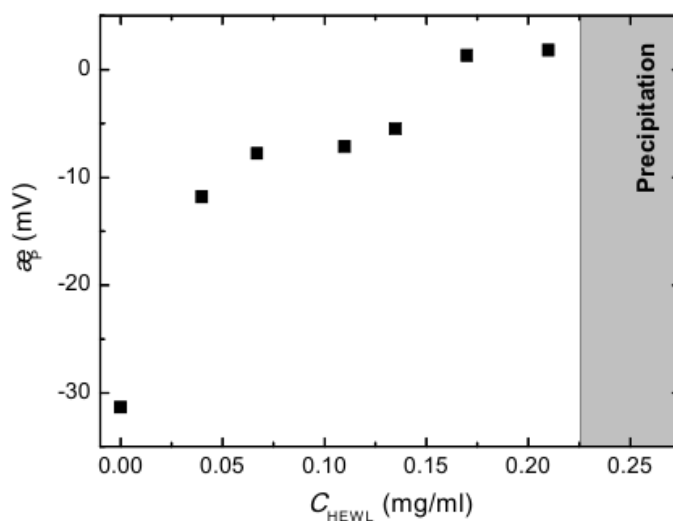


Figure 5. Zeta potential, ζ_P , as a function of C_{HEWL} , for the solutions of the PtBS-SCPI/HEWL system at pH 7 and 0.01 N ionic strength.

In order to obtain information regarding the effective charge of the complexes, electrophoretic light scattering (ELS) measurements were performed on the same series of solutions of the PtBS-SCPI/HEWL system at pH 7 and 0.01M ionic strength.

The measured values of the zeta potential, ζ_P , for the solutions of the complexes as a function of C_{HEWL} are presented in Figure 5.

As it can be seen, ζ_P decreases in absolute value as the concentration of the protein increases, or equivalently the effective negative charge of the complexes is reduced as a function of protein concentration.

This change is in agreement with the notion that as the number of protein molecules interacting with each polyelectrolyte chain of the corona of the micelles increases, the degree of neutralization of the SCPI block negative charges becomes higher and thus the effective charge of the complexes decreases.

Finally, atomic force microscopy (AFM) measurements provided additional information regarding the structure of the complexes. Figure 6 shows two AFM images with different resolution of the complexes formed at $C_{\text{HEWL}} = 0.17$ mg/ml of the PtBS-SCPI/HEWL system at pH 7 and 0.01 N ionic strength deposited on silicon wafers after evaporation of the solvent.

Although a direct comparison with the corresponding results from DLS measurements is not possible, due to the different state of the complexes (dry state in AFM measurements vs. solvated state in DLS measurements), some conclusions about their structure can be drawn. As it can be seen, assemblies of nearly spherical shape are discerned in both images with planar dimensions of about 100 – 200 nm, while their height ranges from 20 to 40 nm.

The observed spherical shape is in agreement with the results from light scattering measurements. The observed dimensions, in regard to the corresponding hydrodynamic size in solution, support the notion that the formed nanostructures adopt a more collapsed structure upon deposition.

Nevertheless, the assemblies seen in higher resolution (right image) seem to have a complicated internal structure, which probably stems from the fact that at this protein concentration supramicellar aggregates of individual polyelectrolyte micelles complexed with protein molecules are formed in the solution. It is the presence of several micelles within the same aggregate that results in the observed morphology and this should be attributed to the characteristics of the hard spherical cores of the micelles and the loose mixed polyelectrolyte/protein corona of the complexes.

Apparently, these supramicellar aggregates are characterized by a rather loose structure, able to deform to some extent upon surface deposition and after solvent evaporation. Nevertheless, complexation sites with protein molecules within the micellar coronas may act as crosslinks that allow the aggregates to retain their spherical overall shape (at least partially).

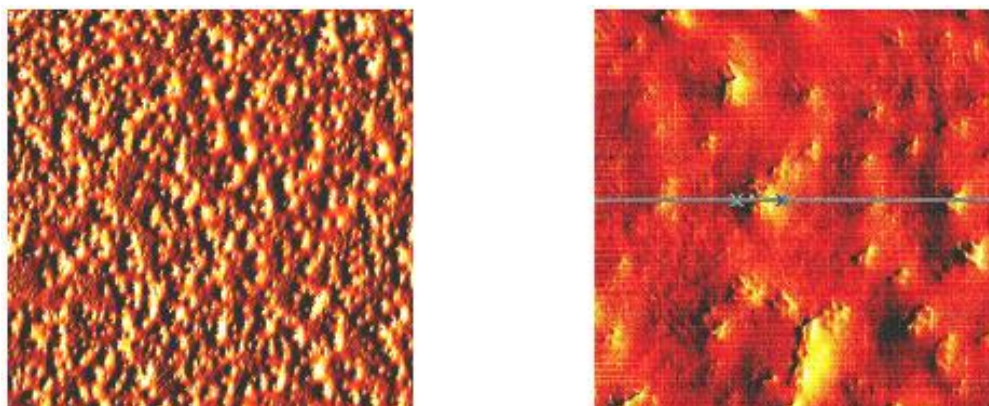


Figure 6. Atomic force microscopy images of complexes formed at $C_{\text{HEWL}} = 0.17$ mg/ml of the PtBS-SCPI/HEWL system at pH 7 and 0.01 N ionic strength on silicon wafers. Bars represent 1 μm (left) and 200 nm (right) respectively.

3.3. Effect of Ionic Strength

The increase of the ionic strength in the solutions of the complexes is expected to influence greatly the solution behavior and structure of the preformed complexes since it induces charge screening and weakening of the electrostatic interactions. This effect was investigated by means of DLS measurements at 0.1 and 0.5 N ionic strength. The resulting I_{90} , R_h and PDI values (from measurements at 90°) for the solutions of the PtBS-SCPI/HEWL system at pH 7 are shown in Figure 7 as a function of C_{HEWL} . The corresponding values at 0.01 N ionic strength are also included for comparison.

Apparently, as the ionic strength of the solution increases the mass of the preformed complexes, which is proportional to I_{90} , decreases. At the same time their size is almost constant, except from the case of the complexes at higher C_{HEWL} values and 0.5 N ionic strength where an increase is observed. Finally, the polydispersity of the system seems to be unaffected from the initial increase of the ionic strength at 0.1 N, while further increase to 0.5 N results in higher PDI values.

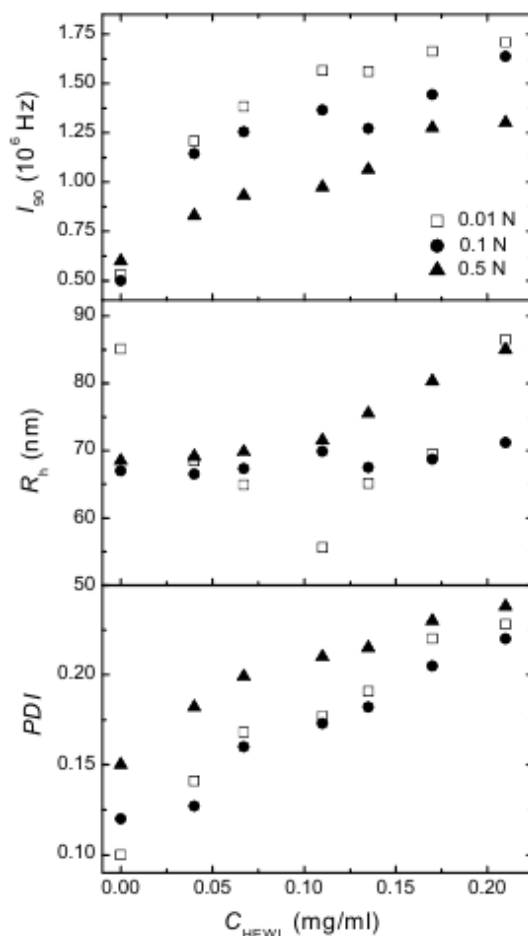


Figure 7. Light scattering intensity at 90° , I_{90} , hydrodynamic radius, R_h , and polydispersity index, PDI , as a function of C_{HEWL} , for the solutions of the PtBS-SCPI/HEWL system at pH 7 and 0.1 and 0.5 N ionic strength. The corresponding values at 0.01 N ionic strength are included for comparison.

From the observed changes it can be concluded that alterations in the ionic strength of the solution influences the structure of the preformed block polyelectrolyte/protein complexes at low ionic strength. Screening of ionic interactions results in complexes of lower mass as ionic strength increases. Hydrodynamic dimensions of the complexes depend on the ratio of the components as well as the actual ionic strength of the medium. Larger polydispersities are observed at 0.5 N probably due to some decomplexation of the initial aggregates as a result of the increased ionic strength that weakens appreciably ionic interactions. In summary, it can be concluded that the ratio of the two components and the ionic strength of the solution can be used as independent factor in order to fine tune and control the structure of the complexes.

3.4. Protein Structure within the Complexes

The preservation of enzymatic activity, which is directly correlated with the actual conformation of the protein in the complexes, is a key factor in most potential applications involving protein-polyelectrolyte complexes. Therefore, fluorescence and infrared spectroscopic measurements were conducted so as to investigate the structure of the complexed protein.

In the first place, three representative solutions at $C_{\text{HEWL}} = 0.04, 0.11$ and 0.17 mg/ml of the PtBS-SCPI/HEWL system at pH 7 and 0.01 N ionic strength were investigated by means of fluorescence spectroscopy. The measured spectra are shown in Figure 8, along with the corresponding spectrum of a neat HEWL solution at 0.5 mg/ml concentration for comparison. In spite of the observed intensity variation, which stems from the difference in the protein concentration, the general spectral characteristics of the neat protein are preserved and all spectra exhibit a maximum around 340 nm. Thus it can be concluded that no protein denaturation is observed upon complexation [40, 41], since that would result in a significant shift in λ_{max} and some broadening of the fluorescence peak of the protein.

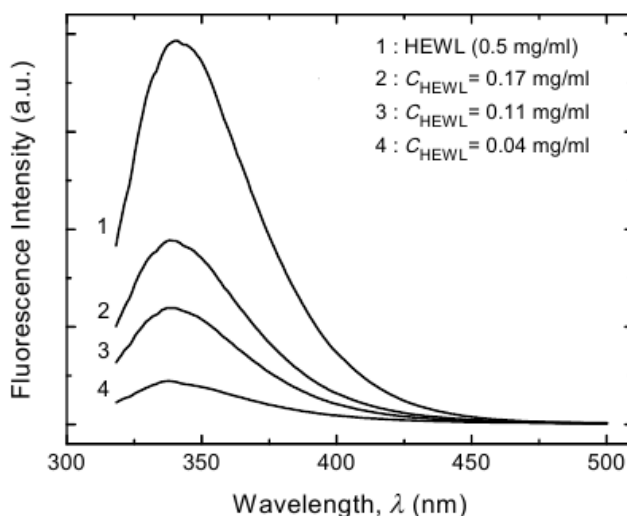


Figure 8. Fluorescence spectra of three representative solutions at $C_{\text{HEWL}} = 0.04, 0.11$ and 0.17 mg/ml of the PtBS-SCPI/HEWL system at pH 7 and 0.01 N ionic strength. The spectrum of neat HEWL at 0.5 mg/ml concentration is included for comparison.

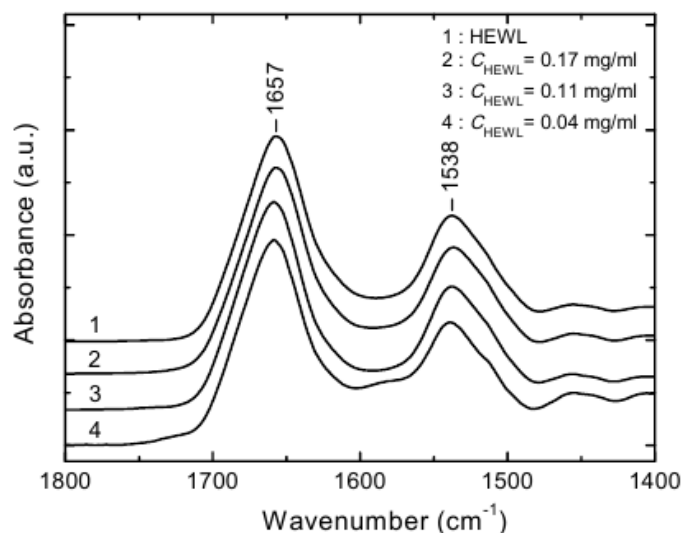


Figure 9. Infrared spectra in the Amide I and II region of three representative solutions at $C_{\text{HEWL}} = 0.04$, 0.11 and 0.17 mg/ml of the PtBS-SCPI/HEWL system at pH 7 and 0.01 N ionic strength. The corresponding spectrum of neat HEWL is included for comparison.

In addition, infrared spectroscopy measurements were performed and Figure 9 shows the IR spectra of the same representative solutions ($C_{\text{HEWL}} = 0.04$, 0.11 and 0.17 mg/ml) of the PtBS-SCPI/HEWL system at pH 7 and 0.01 N ionic strength in the Amide I and II region, including the corresponding spectrum of neat HEWL for comparison. The spectra have been normalized to the intensity of the Amide I band, after subtraction of the spectral contribution of the neat polyelectrolyte diblock copolymer. The constancy of the Amide I and II profiles, peaking at about 1657 and 1538 cm^{-1} respectively, indicates the absence of significant protein configuration changes, such as those observed upon denaturation [42, 43], even in the case of complexes in the solid state.

CONCLUSION

This study focuses on the electrostatic complexation process between the star-like polyelectrolyte micelles formed by the self-assembly of poly(*tert*-butylstyrene)-*b*-poly(sodium(sulfamate-carboxylate)isoprene) (PtBS-SCPI) amphiphilic diblock copolymer in water and the protein lysozyme (HEWL). It was shown that the structure and solution behavior of the formed complexes depend on the ratio of the two components. The interaction of the protein molecules with the polyelectrolyte chains of the corona of the micelles causes the neutralization of the opposite charges of the system, which in turn results in the shrinking of the polyelectrolyte corona and the reduction of the solubility of the micelles complexed with protein. These effects become more dominant as the number of interacting protein molecules per polyelectrolyte chain increases, leading to the aggregation of the complexed micelles and eventually the precipitation of the micelle/protein complexes. The increase of the ionic strength of the solution results in complexes of lower mass due to partial dissociation of the initial aggregates. Moreover, light scattering measurements together with

atomic force microscopy imaging show that the complexes possess a nearly spherical shape. Finally, spectroscopic measurements revealed that the protein structure is preserved upon complexation. This investigation shows that it is possible to form hybrid synthetic/biological nanostructures in aqueous solutions via the electrostatic interaction of preformed block polyelectrolyte micelles and proteins (particularly enzymes). A number of parameters including block copolymer and micellar characteristics, as well as the ratio of the components and solution ionic strength can be utilized in order to control the characteristics of the particular chimeric nanostructures. Their utilization in a number of possible application oriented fields, including protein drug delivery, enzymatic nanocatalysis and functional surface modification remain to be investigated in the near future.

ACKNOWLEDGMENTS

Authors acknowledge financial support of the work by the NANOMACRO 1129 project which is implemented in the framework of the Operational Program “Education and Life-long Learning” (Action “ARISTEIA I”) and it is co-funded by the European Union (European Social Fund) and by national funds.

REFERENCES

- [1] Moffitt, M.; Khougaz, K.; Eisenberg, A. *Acc. Chem. Res.* 1996, 29, 95-102.
- [2] Kötz, J.; Kosmella, S.; Beitz, T. *Prog. Polym. Sci.* 2001, 26, 1199-1232.
- [3] Förster, S.; Abetz, V.; Müller, A. H. E. *Adv. Polym. Sci.* 2004, 166, 173-210.
- [4] Cohen Stuart, M. A.; Hofs, B.; Voets, I. K.; de Keizer, A. *Curr. Opin. Colloid Interface Sci.* 2005, 10, 30-36.
- [5] Hales, K.; Pochan, D. J. *Curr. Opin. Colloid Interface Sci.* 2006, 11, 330-336.
- [6] Pergushov, D. V.; Borisov, O. V.; Zezin, A. B.; Müller, A. H. E. *Adv. Polym. Sci.* 2011, 241, 131-161.
- [7] Talingting, M. R.; Voigt, U.; Munk, P.; Webber, S. E. *Macromolecules* 2000, 33, 9612-9619.
- [8] Pergushov, D. V.; Remizova, E. V.; Feldthusen, J.; Zezin, A. B.; Müller, A. H. E.; Kabanov, V. A. *J. Phys. Chem. B* 2003, 107, 8093-8096.
- [9] Lysenko, E. A.; Chelushkin, P. S.; Bronich, T. K.; Eisenberg, A.; Kabanov, V. A.; Kabanov, A. V. *J. Phys. Chem. B* 2004, 108, 12352-12359.
- [10] Pergushov, D. V.; Remizova, E. V.; Gradzielski, M.; Lindner, P.; Feldthusen, J.; Zezin, A. B.; Müller, A. H. E.; Kabanov, V. A. *Polymer* 2004, 45, 367-378.
- [11] Matějčiček, P.; Uchman, M.; Lokajová, J.; Štěpánek, M.; Procházka, K.; Špírková, M. *J. Phys. Chem. B* 2007, 111, 8394-8401.
- [12] Kulebyakina, A. I.; Lysenko, E. A.; Chelushkin, P. S.; Kabanov, A. V.; Zezin, A. B. *Polym. Sci., Ser. A* 2010, 52, 574-585.
- [13] Zhang, W.; Shi, L.; Gao, L.; An, Y.; Wu, K. *Macromol. Rapid Commun.* 2005, 26, 1341-1345.

-
- [14] Zhang, W.; Shi, L.; Miao, Z.-J.; Wu, K.; An, Y. *Macromol. Chem. Phys.* 2005, 206, 2354-2361.
- [15] Masci, G.; De Santis, S.; Cametti, C. *J. Phys. Chem. B* 2011, 115, 2196-2204.
- [16] Tribet, C. *Physical Chemistry of Polyelectrolytes*, ed. Radeva, T., Marcel & Dekker, New York, 2001, ch. 19, pp. 687-741.
- [17] Cooper, C. L.; Dubin, P. L.; Kayitmazer, A. B.; Turksen, S. *Curr. Opin. Coll. Interface Sci.* 2005, 10, 52-78.
- [18] Harada, A.; Kataoka, K. *Langmuir* 1999, 15, 4208-4212.
- [19] Lindhoud, S.; de Vries, R.; Norde, W.; Cohen Stuart, M. A. *Biomacromolecules* 2007, 8, 2219-2227.
- [20] Lindhoud, S.; Norde, W.; Cohen Stuart, M. A. *J. Phys. Chem. B* 2009, 113, 5431-5439.
- [21] Pispas, S. *J. Polym. Sci., Part A: Polym. Chem.* 2007, 45, 509-520.
- [22] Gao, G.; Yan, Y.; Pispas, S.; Yao, P. *Macromol. Biosci.* 2010, 10, 139-146.
- [23] Schmidt, V.; Giacomelli, C.; Lecolley, F.; Lai-Kee-Him, J.; Brisson, A. R.; Borsali, R. *J. Am. Chem. Soc.* 2006, 128, 9010-9011.
- [24] Schmidt, V.; Giacomelli, C.; Brisson, A. R.; Borsali, R. *Mater. Sci. Eng., C* 2008, 28, 479-488.
- [25] Schmidt, V.; Giacomelli, C.; Gounou, C.; Lai-Kee-Him, J.; Brisson, A. R.; Borsali, R. *Langmuir*, 2008, 24, 12189-12195.
- [26] Karayianni, M.; Pispas, S. *Soft Matter*, 2012, 8, 8758-8769.
- [27] Wittemann, A.; Haupt, B.; Ballauff, M. *Progr. Colloid Polym. Sci.* 2006, 133, 58-64.
- [28] Henzler, K.; Wittemann, A.; Breininger, E.; Ballauff, M.; Rosenfeldt, S. *Biomacromolecules*, 2007, 8, 3674-3681.
- [29] Henzler, K.; Haupt, B.; Rosenfeldt, S.; Harnau, L.; Narayanan, T.; Ballauff, M. *Phys. Chem. Chem. Phys.* 2011, 13, 17599-17605.
- [30] Karayianni, M.; Mountrichas, G.; Pispas, S. *J. Phys. Chem. B* 2010, 114, 10748-10755.
- [31] Tanford, C.; Roxby, R. *Biochemistry* 1972, 11, 2192-2198.
- [32] Kuehner, D. E.; Engmann, J.; Fergg, F.; Wernick, M.; Blanch, H. W.; Prausnitz, J. M. *J. Phys. Chem. B* 1999, 103, 1368-1374.
- [33] Pispas, S. *J. Polym. Sci., Part A: Polym. Chem.* 2006, 44, 606-613.
- [34] Gebelein, C. G.; Murphy, D. *Advances in Biomedical Polymers*, ed. Gebelein, C. G., Plenum Press, New York, 1985, pp 277-284.
- [35] van der Does, L.; Beugeling, T.; Froehling, P. E.; Bantjes, A. *J. Polym. Sci., Polym. Symp.* 1979, 66, 337-348.
- [36] Huglin, M. B. *Light Scattering from Polymer Solutions*, Academic Press, New York, 1972.
- [37] Chu, B. *Laser Light Scattering: Basic Principles and Practice*, Academic Press, New York, 1991.
- [38] Förster, S.; Zisenis, M.; Wenz, E.; Antonietti, M. *J. Chem. Phys.* 1996, 104, 9956-9970.
- [39] Qin, A.; Tian, M.; Ramireddy, C.; Webber, S. E.; Munk, P.; Tuzar, Z. *Macromolecules* 1994, 27, 120-126.
- [40] Sato, T.; Mattison, K. W.; Dubin, P. L.; Kamachi, M.; Morishima, Y. *Langmuir* 1998, 14, 5430-5437.
- [41] Nishimoto, E.; Yamashita, S.; Yamasaki, N.; Imoto, T. *Biosci. Biotechnol. Biochem.* 1999, 63, 329-336.

- [42] Lad, M. D.; Ledger, V. M.; Briggs, B.; Green, R. J.; Frazier, R. A. *Langmuir* 2003, 19, 5098-5103.
- [43] Smeller, L.; Meersman, F.; Heremans, K. *Biochim. Biophys. Acta* 2006, 1764, 497-505.

S. E.